Estimating the Fraction of Photosynthetically Available Radiation Absorbed by Live Phytoplankton from MODIS and VIIRS Data

R. Frouin, <u>J. Tan</u>

Scripps Institution of Oceanography, University of California San Diego, La Jolla, California, USA

Introduction

-APAR is an important parameter for estimating primary production (PP).

PP = e APAR PAR

where *PAR* is the photosynthetically available radiation (below the surface), *APAR* is the fraction of PAR absorbed by live phytoplankton, and *e* is an efficiency factor for photosynthesis.

-APAR can be expressed as (Kirk 1994):

$APAR = \int\int\{K_d(\lambda,z)E_d(\lambda,z)\,a_{ph}(\lambda,z)/a_{tot}(\lambda,z)\}d\lambda \,/ \int E_d(\lambda,0^-)\,d\lambda$

where K_d is the diffuse attenuation coefficients, E_d is the spectral solar irradiance below the surface, a_{ph} is the phytoplankton absorption coefficient, a_{tot} is the total absorption coefficient, and the integral is over the PAR spectral range, i.e., 400 to 700 nm, and over the depth z (from surface to the depth of the euphotic zone).

$APAR = \int(E_d(\lambda)\,a_{ph}(\lambda)/a_{tot}(\lambda))d\lambda \,/ \int E_d(\lambda)d\lambda$, *if homogenous ocean*

-Computing APAR requires knowledge of $K_d(\lambda)$, $E_d(\lambda)$, $a_{ph}(\lambda)$, and $a_{tot}(\lambda)$.

-The above water irradiance can be obtained by adapting existing methods for *PAR* above the surface. This is straightforward since the effect of clouds on transmittance is white in the PAR spectral range.

-The passage below the surface can be accomplished by multiplying the above water irradiance by $(1 - R_g)[1 - R_w(\lambda)]$ where R_g is the surface reflectance (due to Fresnel reflection) and R_w the marine reflectance (due to backscattering by the water body).

-The absorption coefficients $a_p(\lambda)$ and $a_{tot}(\lambda)$ can be obtained using various techniques (see, for example, IOCCG, 2005).

-Estimating *[chl]* or a_p and a_{tot} from $R_w(\lambda)$ is accomplished with uncertainties (it is especially difficult to estimate a_p).

Methodology

-APAR can be re-expressed in terms of R_w as:

$$APAR \approx \int \{E_d(0^-) \, [a_{ph}/(a_{ph} + a_{dm} + a_g)] \, [1 - (R_w(0^-)/R_{w0}(0^-))(f_0/f)(b_{b0}/(b_{b0} + b_{bp}))] \} d\lambda \, / \int E_d(0^-) \, d\lambda$$

by incorporating the following equations:

$$a_{tot} = a_{ph} + a_{dm} + a_g + a_0, \quad R_{w0}(0^-) \approx f_0 b_{b0}/a_0, \quad R_w(0^-) \approx f b_b/a_{tot}$$

where a_{dm}, a_g and a_0 are the absorption coefficients by detritus/sediments, colored dissolved organic matter, and pure water, respectively, b_{b0} and b_{bp} are the backscattering coefficients for water molecules and particles, respectively, and R_{w0} is the marine reflectance for pure sea water.

-**This expression suggests that APAR can be approximated by a linear combination of marine reflectance in the PAR spectral range**, especially when the backscattering coefficient for hydrosols can be considered small compared with the one for molecules (case of clear waters).

Algorithm Development/Optimization

-A representative ensemble of the synthetic and in situ data sets of $APAR$ and $R_w(0^-)$ will be generated, with two sub-ensembles, statistically similar, for establishing the algorithm and for validation, respectively.

-Realistic uncertainties will be assigned to $R_w(0^-)$ following Moore et al. (2009) and Jackson et al. (2017) by (1) determining the errors for each water class based on the match-up data sets of satellite-derived and measured water reflectance and (2) finding membership to the classes and applying proper weights.

-The wavelengths will be selected to maximize the sensitivity to $APAR$, minimize the influence of noise on $R_w(0^-)$, and minimize the influence of b_{bp} and $a_g + a_{dm}$ on the linear equation, by systematically examining the performance of regressing $APAR$ versus the linear combination of $R_w(0^-)/R_{w0}(0^-)$ for any combination of wavelengths possible.

Algorithm Development/Optimization (cont)

-Linear combinations will also be determined for each of the water class, a procedure that might provide more accurate results. Then the APAR estimates will be a weighted average calculated from the individual linear combinations according to the membership to the water classes.

-Impact of vertical heterogeneity on performance will be assessed.

-Performance degradation due to noise will be quantified by comparing results obtained on noisy and non-noisy ensembles.

-Linear combinations will also be established for $R_w(0^-)/R_{w0}(0^-)$ at zero solar zenith angle for possible use with normalized ratios.

-Comparisons will be made with methods using [chl] in a power law or using absorption coefficients by inversion schemes (e.g. QAA, GSM, GIOP).

Uncertainty Assignment

-Associating uncertainties to the APAR products (level 2 and 3) will be done on a pixel-by-pixel basis using the water-class method, which has been adopted for operationally characterizing the uncertainty of OC-CCI products.

-The estimated and prescribed APAR data sets will be used to generate the uncertainty metrics, i.e. bias and RMS, for each water class, using the noisy ensemble.

-The fuzzy membership for each MODIS/VIIRS water reflectance retrieval at pixel level will be determined and used to calculate the APAR uncertainties using weights according to membership.

-In the end, a RMS difference and a bias will be associated to each Level-2 PAR estimate.

Uncertainty Assignment (cont)

-The binned Level-3 products will be obtained by accumulating and averaging individual Level-2 pixels into well defined spatial and temporal bins, i.e., 1 day, 8 days, calendar month, calendar year, and approximately 4.64 km resolution.

-The uncertainties of binned Level 3 APAR products can be calculated as:

$$\Delta_j = [(1/N)\Sigma(\Delta_{jk})^2]^{0.5} \qquad\qquad m_j=(1/N)\Sigma m_{jk}$$

where Δ_{jk} and m_{jk} characterize the RMS and bias on the level 2 pixel k of bin j, N is the number of pixel in bin j, and the sum is over k.

Feasibility

Figure 1: Dependence of APAR on [chl] and $R_w(0-)/R_{w0}(0-)$ for typical Case 1 waters, vertically homogeneous (blue) and heterogeneous (red). Solar zenith angle is 30° (solid line) and 60° (dashed line).
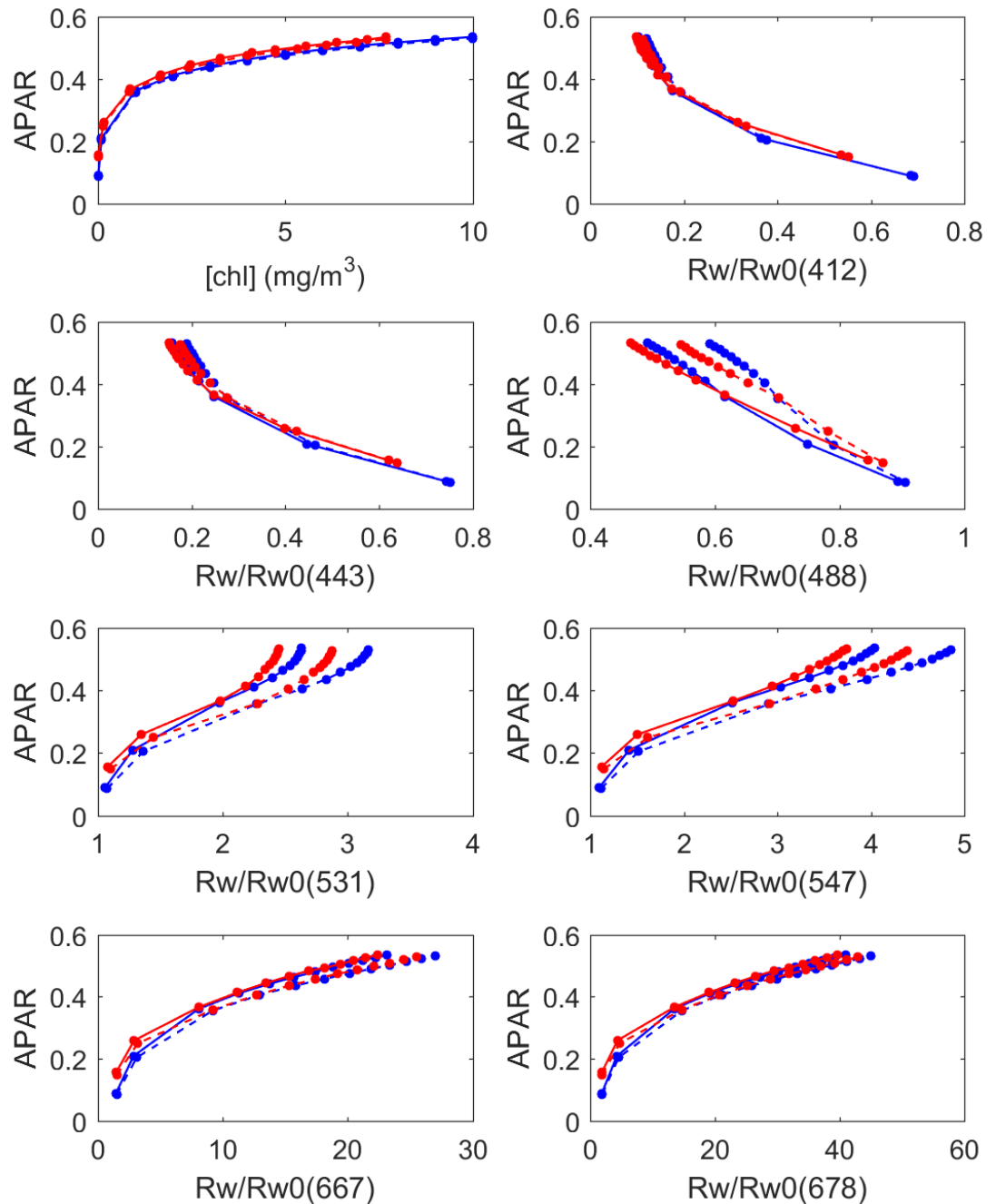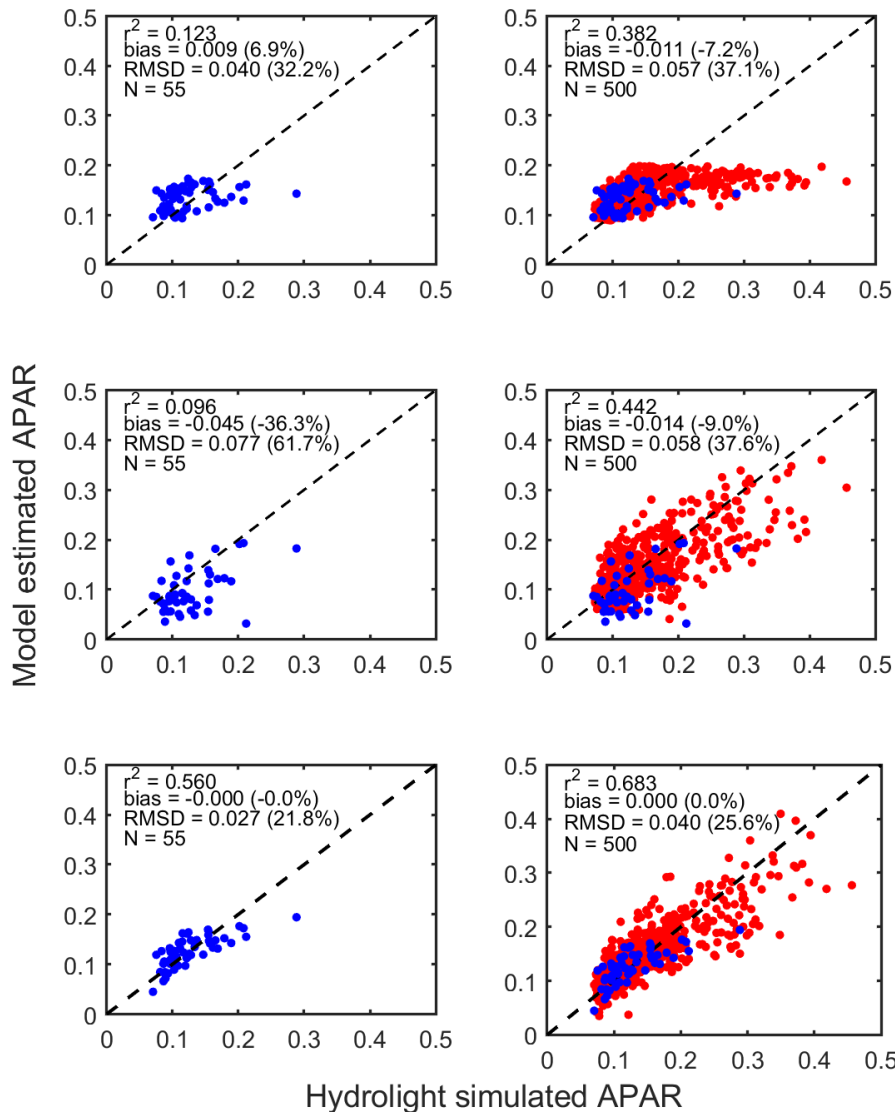
		[chl] based	QAA based	R_w/R_{w0} ratios
	R^2	0.123	0.096	0.56
Case 1, N=55	bias (%)	0.009 (6.9%)	-0.045 (-36.3%)	-0.0 (0.0%)
	RMSD (%)	0.040 (32.2%)	0.077 (61.7%)	0.027 (21.8%)
	R^2	0.392	0.473	0.689
Case 2, N=445	bias (%)	-0.014 (-8.5%)	-0.010 (-6.3%)	-0.000 (-0.0%)
	RMSD (%)	0.059 (37.4%)	0.055 (35.0%)	0.040 (25.4%)

Figure 2: *Comparison of estimated and theoretical (Hydrolight simulated) APAR for Case 1 waters (left) and Case 1 + Case 2 waters (right). Data set is from IOCCG (2006). Top row: using OCM3-derived [chl], middle row: using QAA-derived a_{ph} and a_{tot}, and bottom row: using R_w/R_{w0} ratios.*
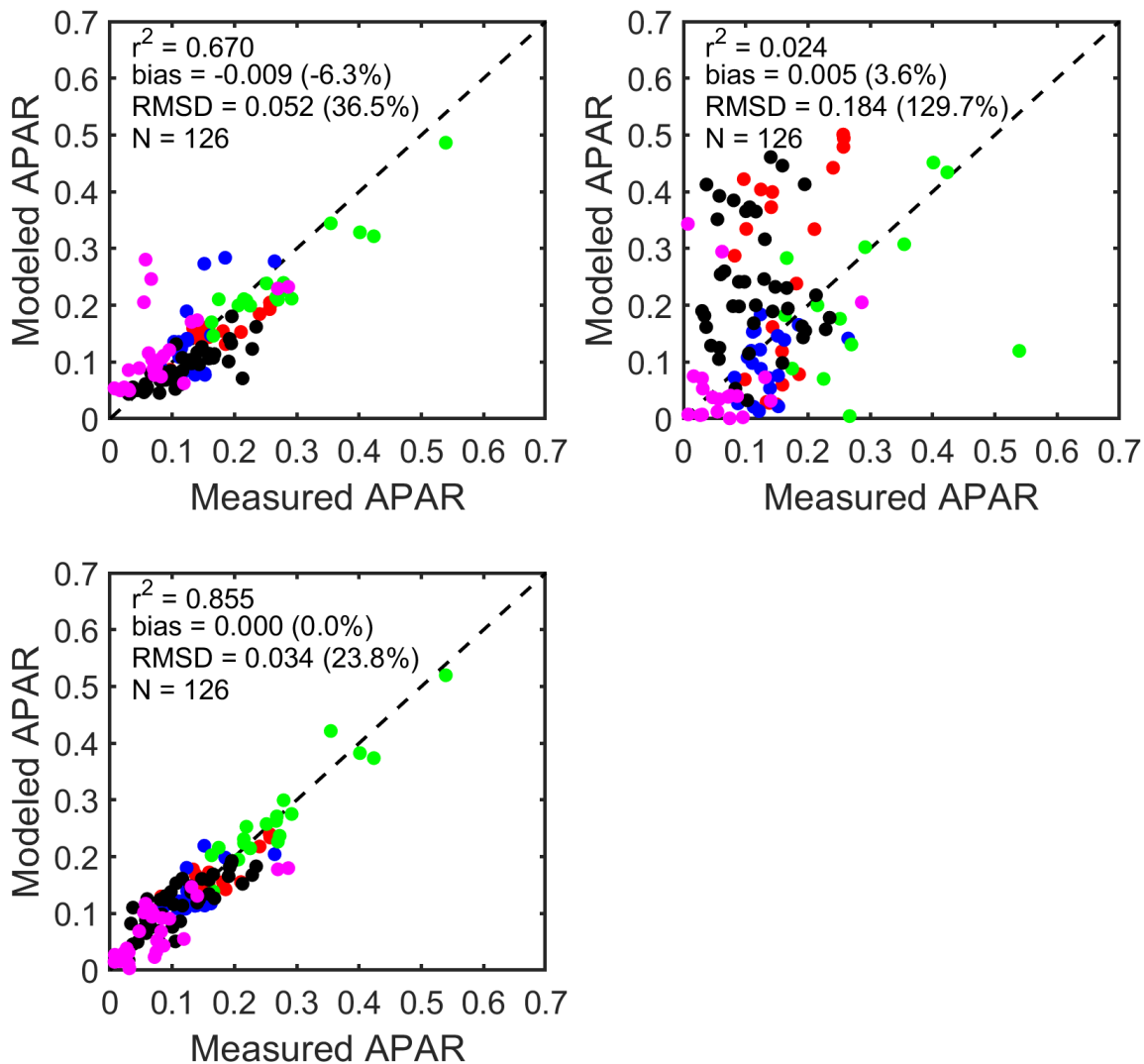
Figure 3: *Comparison of estimated and "measured" APAR using field data collected during OUTPACE (red), BIOSOPE (blue), MV1102 (green), ACE0103 (black) and ICESCAPE2011 (magenta) cruises: Top left - using OC3M derived [chl], top right - using QAA derived a_{ph} and a_{tot}, bottom left - using R_w/R_{w0} ratios.*

Data Sources

-Synthesize data sets will be obtained by running Hydrolight at MODIS and VIIRS wavelengths for a wide range of realistic ocean, atmosphere, and surface conditions, and solar zenith angles.

- The IOPs will be specified as in IOCCG(2006).

- More recent bio-optical models/relationships may be considered, and the variables (i.e., [chl], $a_{ph}*$, a_{dm}/a_{ph} at 440 nm, a_g/a_{ph} at 440 nm, c_{ph}, b_{dm}) will be varied randomly in the range of expected values for natural waters (IOCCG, 2006).

- Inelastic effects will be considered and the IOPs will not only be specified at the wavelengths of interest, but also in the ultraviolet.

- Vertical heterogeneity in [chl] (Morel and Berthon , 1989) and IOPs will be considered.

Data Sources (cont)

-In situ data sets

- The Scripps Photobiology Group (SPG) database contains one of the best, most comprehensive, globally distributed, and highest quality data sets for ocean color algorithm development and validation.
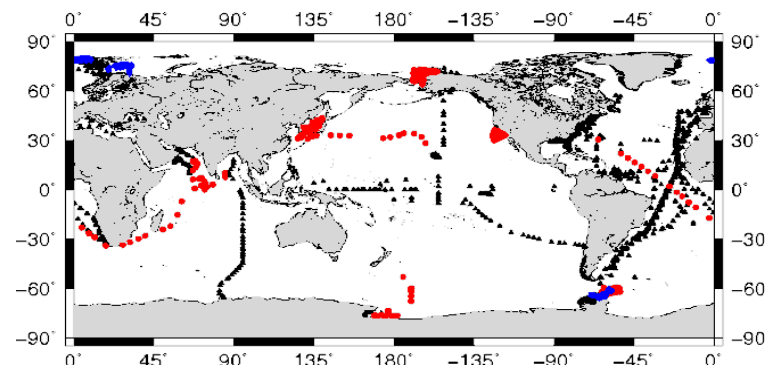
Water Samples	# Samples
ap	7616
as	6001
CHN	3955
Coulter Counter	679
Cyanobacteria	316
Nutrients	4375
Pigments Fluor	19703
Pigments HPLC	6416
PvE	1093
TSM	541

In situ Optics	# Stations
PRR600	76
PRR800	744
MER1012	150
MER2040	310
MER2048	333
SPMR	37
AC9	817
HS6	813
FRRF	452

- Other archives such as SeaBASS and the database created for the validation of the ocean-color products from the ESA Ocean Colour Climate Change Initiative (OC-CCI) (Valente et al., 2016) will be examined.

- Data from other campaigns such as OUTPACE, BIOSOPE, and MV1102 will also be used.

Work Schedule

-Preparation of ensembles for algorithm development. September 2018 to May 2019.

-Optimization of band combination. December 2018 to August 2019.

-Uncertainty assignment to APAR estimates on a pixel by pixel basis. March 2019 to November 2019.

-Development of processing lines and application of the APAR algorithm to MODIS/VIIRS imagery. September 2019 to May 2020.

-Evaluation against in-situ measurements. December 2019 to August 2020.

-Algorithm refinement and adjustment and delivery of final code. March 2020 to November 2020.

Evaluation of PAR products/Generation of consistent long-term time series
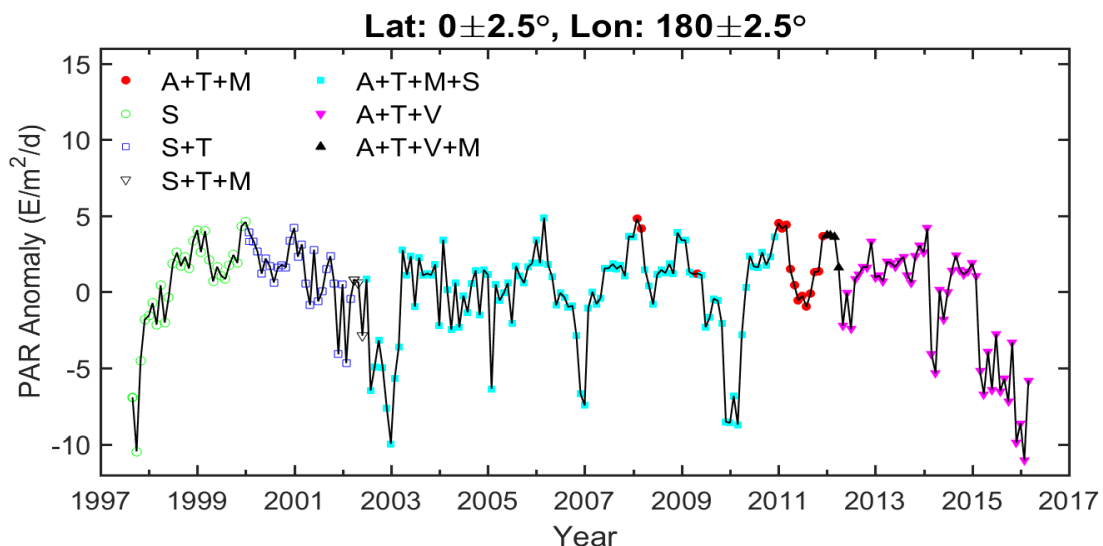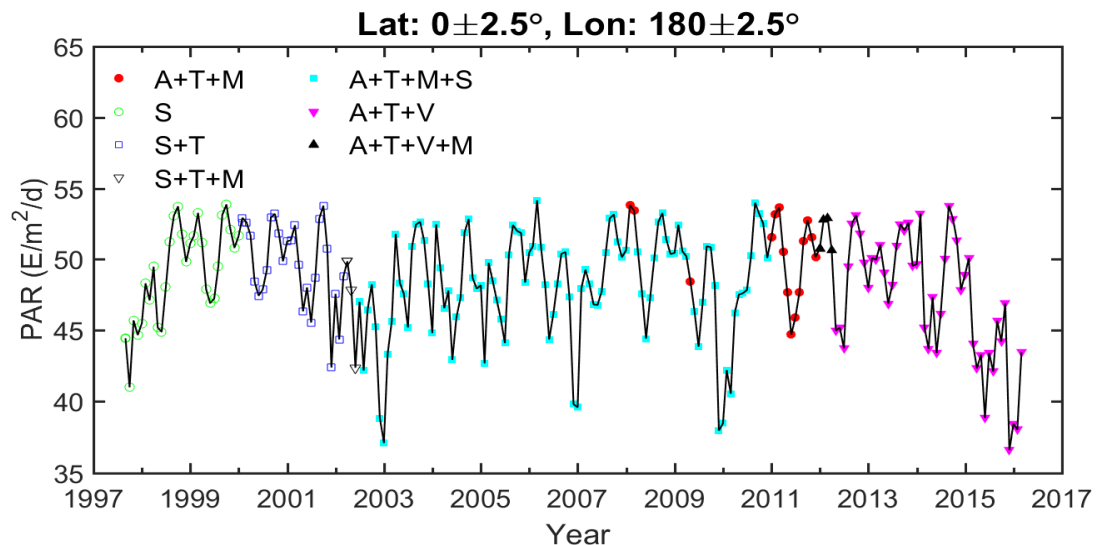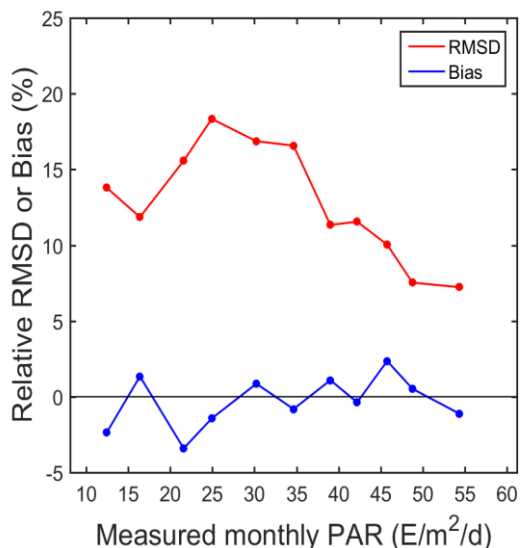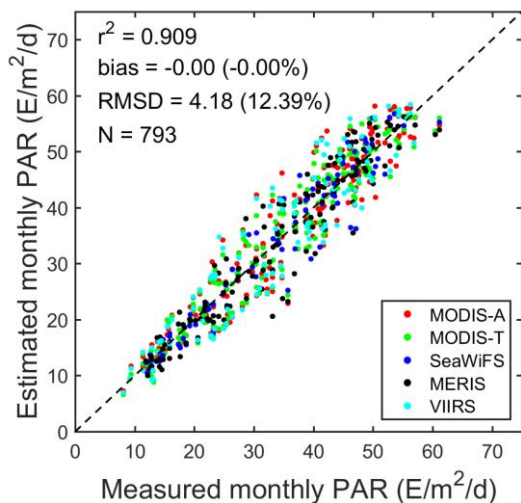
Figure 1: *Left: Comparison between estimated and measured monthly PAR for instruments at four locations: BOUSSOLE, CCE-1 and -2, and COVE. Right: bias and RMSD as a function of PAR.*

Figure 2: *Time series of monthly PAR (top) and PAR anomaly (bottom) in the equatorial Pacific obtained from SeaWiFS (S), MODIS-A (A), MODIS-T (T), MERIS (M), VIIRS (V). The values obtained by individual instruments have been corrected for biases.*

Seasonal and inter-annual PAR variability in the Tropics
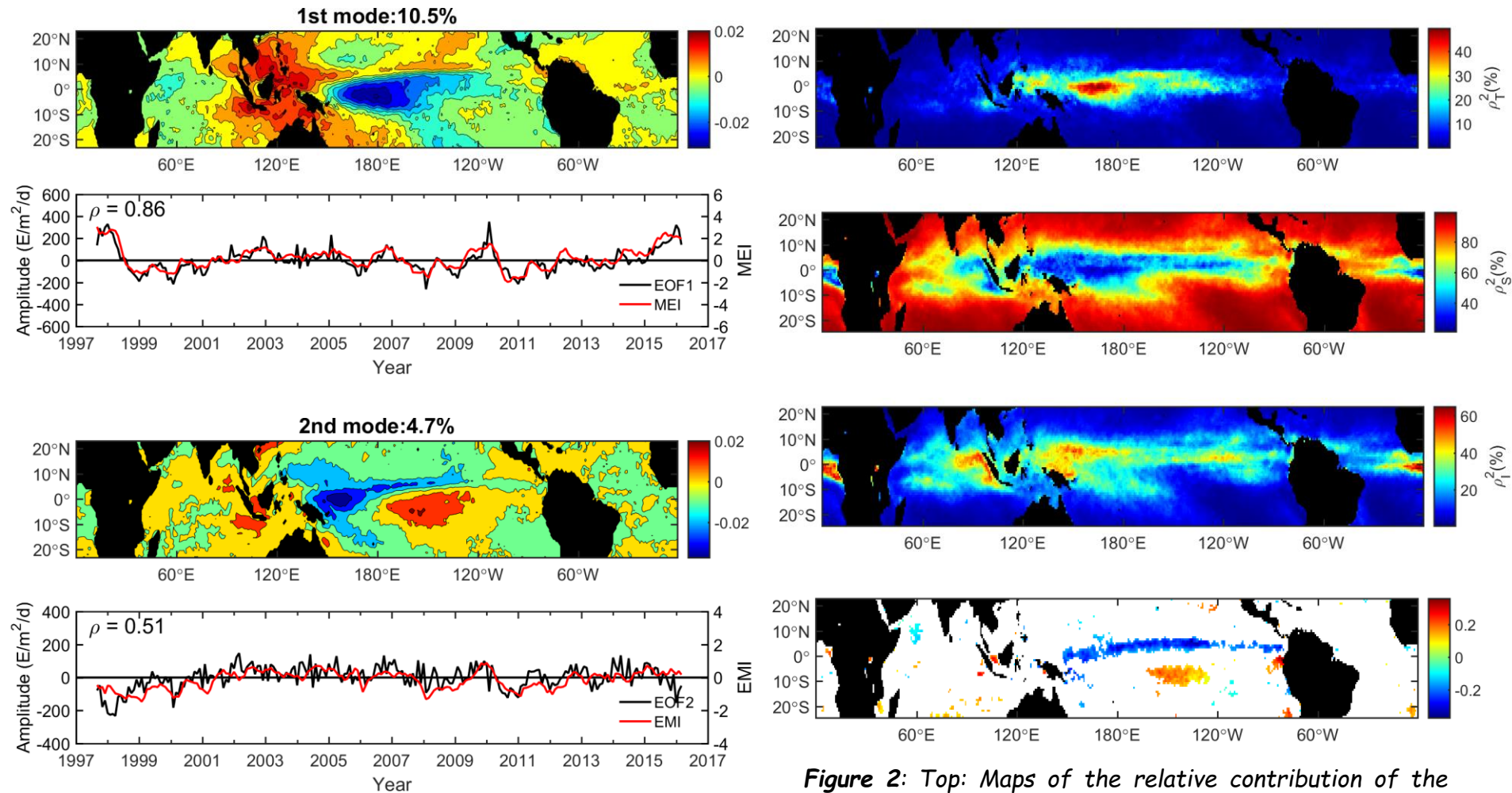
Figure 1: EOF1 and EOF2 and corresponding amplitude time series for the 20-year monthly PAR anomalies. Canonical El Niño Southern Oscillation (ENSO) and Modoki ENSO drive the two leading non-seasonal EOF modes, respectively, with a correlation coefficient of 0.86 between the first mode and the multivariate ENSO Index and of 0.51 between the second mode and the El Nino Modoki Index.

Figure 2: Top: Maps of the relative contribution of the seasonal, the trend, and the irregular component to the total variance of the PAR signal (in %). Bottom: Slope of the linear regression for PAR (in % $year^{-1}$) over 20 years of satellite data. Only statistically significant values ($p<0.05$) are presented PAR decreases significantly (around -0.2 % $year^{-1}$) in the central equatorial and eastern Pacific and increases significantly (around 0.2 % $year^{-1}$) in the central Pacific around latitude 10°S.

Associating uncertainties to satellite PAR products

Daily PAR

Uncertainty (standard deviation)
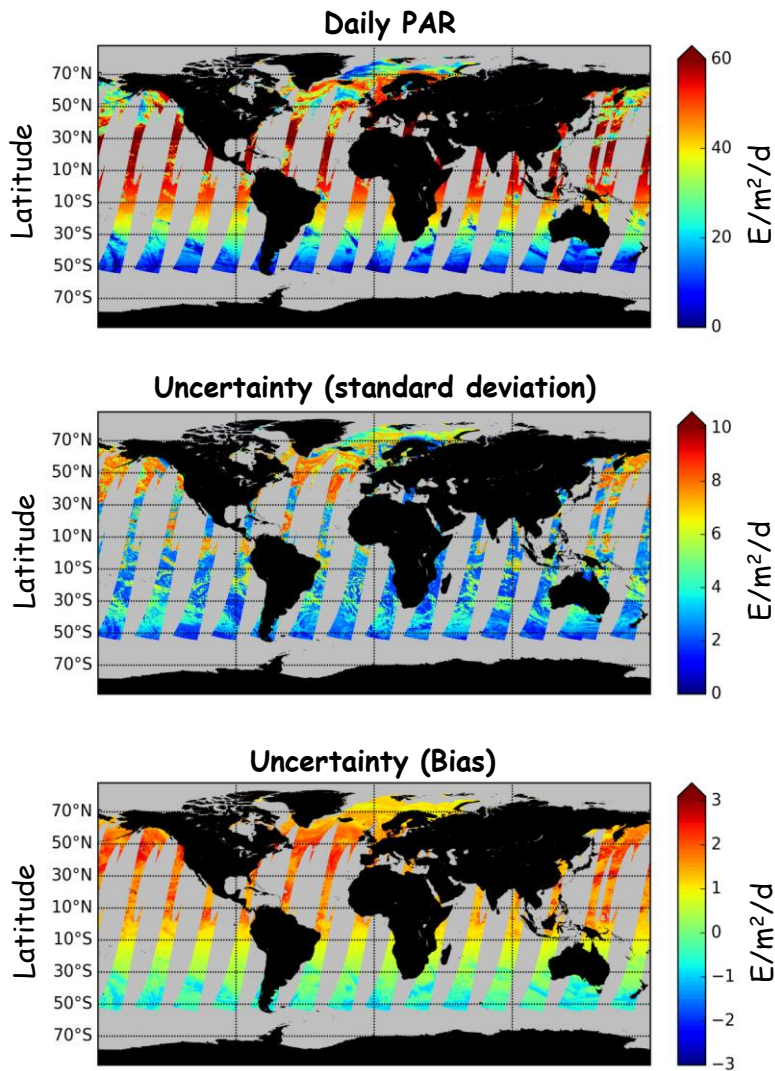
Uncertainty (Bias)

Figure 1: Example of daily PAR product (MERIS, 15 May 2011) with associated algorithm uncertainties (standard deviation, bias). Uncertainties are computed from daily clear sky PAR and cloud factor according to Frouin et al. (Frontiers, 2018).
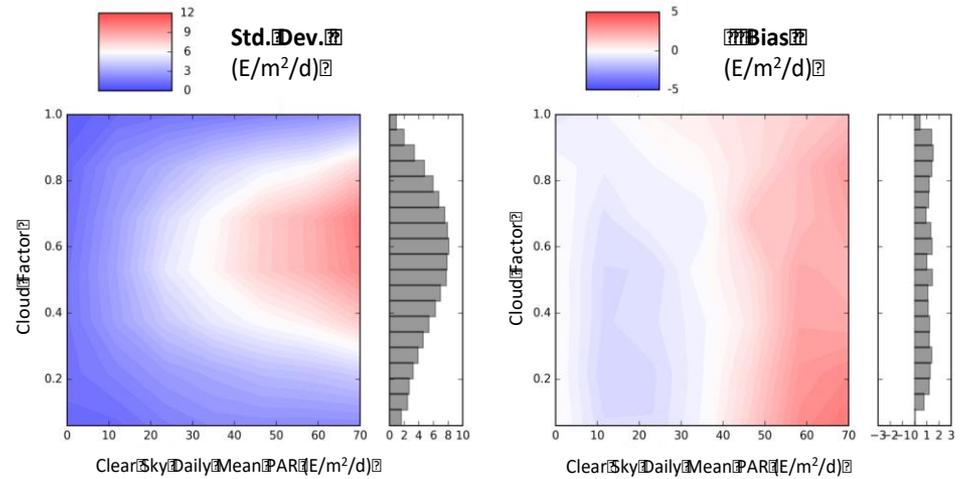
Figure 2: Uncertainty on daily mean PAR above the surface (estimated PAR - actual PAR) from simulations for the period 2003-2012 using 1-hourly resolved MERRA-2 input data. For each day, a set of MERIS TOA spectral reflectance data is simulated for a typical observation at 10:30 UT local time and several viewing geometries (nadir and 20° view zenith angle (VZA) with relative azimuth of 0, 90 and 180°, with sun glint avoidance).
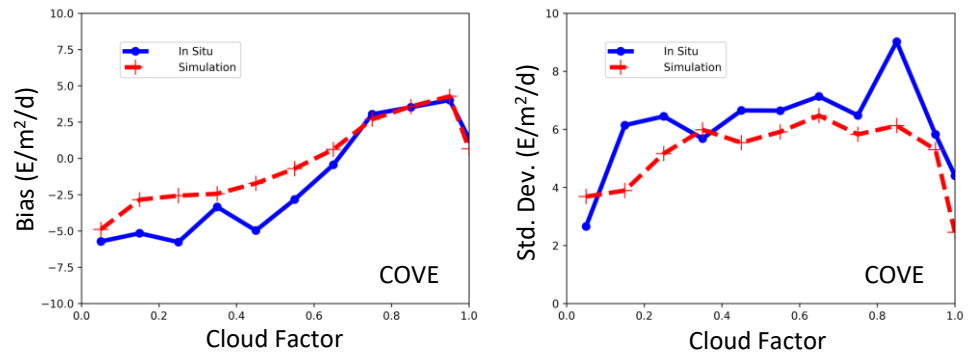
Figure 3: Uncertainties (bias, standard deviation) on MERIS daily mean PAR estimates at the COVE site (Chesapeake Bay). Red curves: using MERRA-2 data (simulation, see text); Blue curves: comparing satellite PAR estimates with in situ measurements.

First Daily Mean PAR Image from EPIC/DSCOVR Data

EPIC-DSCOVR, 01/01/2018
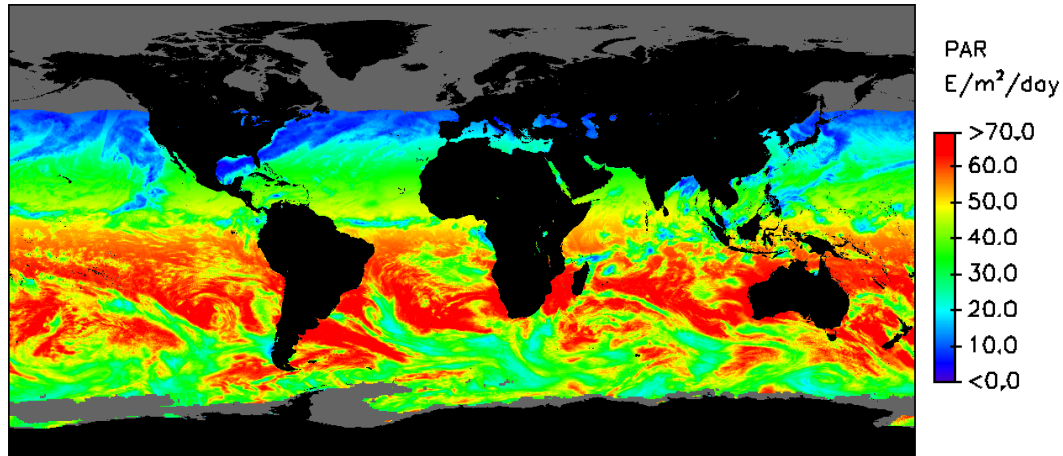
MODIS-Aqua, 01/01/2018
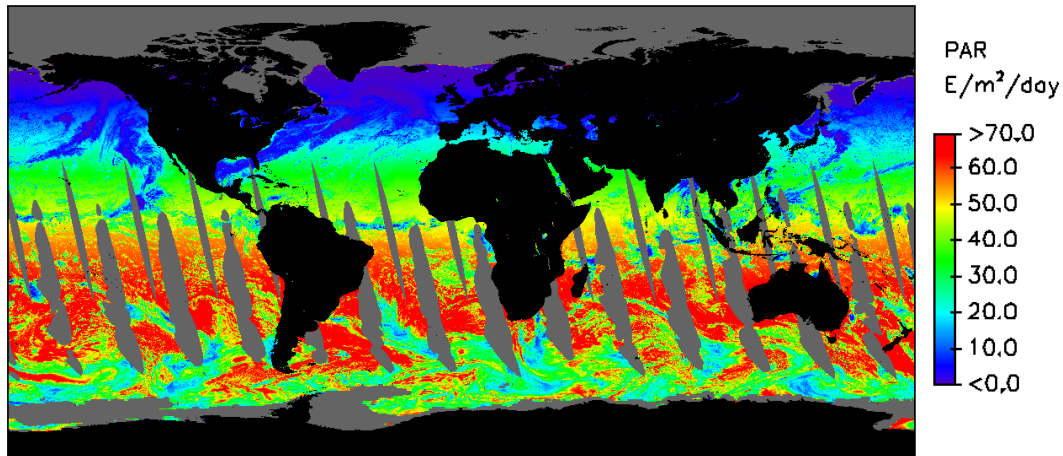
Figure 1: (Top): Image of daily mean PAR at the ocean surface on January 1, 2018 obtained from EPIC/DSCOVR data. (Bottom): Corresponding image generated by the NASA OBPG from MODIS-Aqua data. Land mask is in black and missing data (including ice-contaminated pixels) in grey. Spatial coverage is complete with EPIC at low and middle latitudes, and EPIC PAR image is less noisy than MODIS PAR image.
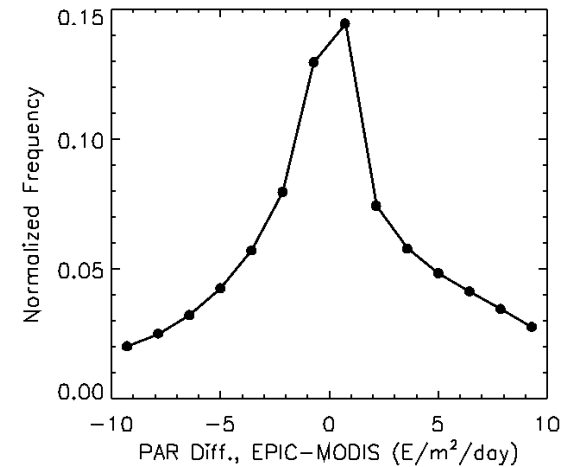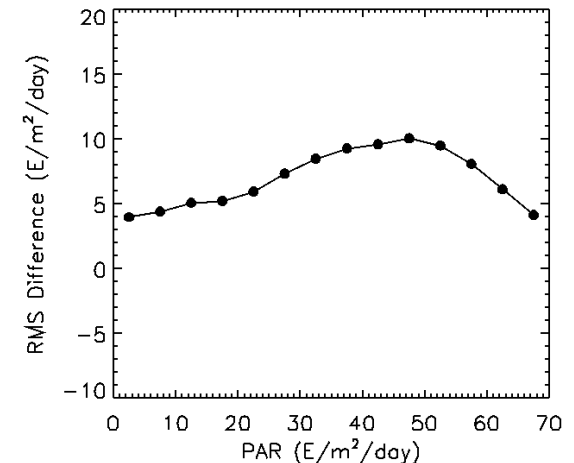
Figure 2: (Top): Histogram of differences between EPIC and MODIS daily mean PAR estimates for January 1, 2018. (Bottom): RMS difference as a function of daily mean EPIC PAR. PAR diffs. are mostly between ±5 E/m²/day and RMS diff. varies between 5 and 10 E/m²/day depending on PAR level.